Performance Comparison of UWB Impulse-Based Multiple Access Schemes in Indoor Multipath Channels

Paul Saad, Cyril Botteron, Roman Merz and Pierre-André Farine
Institute of Microtechnology
University of Neuchâtel, Switzerland
Email: paul.saad@unine.ch

***Abstract*—In this paper, we consider an impulse-based ultra-wideband (UWB) receiver and assess the performance of different multiple access and modulation schemes, including time-hopping pulse position modulation (TH-PPM), time-hopping binary phase shift keying (TH-BPSK), and BPSK-BPSK, under both the additive white Gaussian noise (AWGN) and indoor multipath (CM3) channel assumptions. The assumed receiver combines the received pulses to increase the signal to noise ratio (SNR) and correlates the summed signal with the locally generated template. The performance of the different techniques are estimated using Monte-Carlo simulations and validated by comparing them with the theoretical results obtained for the AWGN channel with the characteristic function (CF) method presented in [1]. Amongst other results, we show that the AWGN channel assumption provides rather optimistic results as compared to the more realistic CM3 indoor channel assumption.**

I. Introduction

UWB is a novel technology emerging in recent years as a promising solution for high speed or low power indoor communications. Indeed, UWB technology offers the potential for robust communications in multipath and multiuser environments, as well as low cost and low complexity implementations. However, the performance of UWB systems is strongly dependant on the multiple access and modulation techniques used. TH multiple access technique, where users are distinguished by their respective pulse arrival time sequences (see, e.g., [2], [3]), is one of the most popular multiple access techniques used for an impulse radio system. For data modulation, different techniques have been studied for UWB impulse signals, such as PPM, BPSK, pulse amplitude modulation (PAM) and on-off keying (OOK) [4]. Nowadays, TH combined with PPM or BPSK is the most common multiple access and modulation scheme. In the literature, an AWGN channel has traditionally been assumed to assess the performance of the different multi-access techniques because it can lead to simple and tractable mathematical models (see, e.g., [1]–[3], [5]–[7]). Unfortunately, an AWGN channel model is a rather optimistic assumption to model real propagation conditions and fading environments for practical UWB systems, as we will show in this paper. To obtain more realistic results, we have thus selected the IEEE 802.15.3a CM3 standard model proposed in [8] as it provided very good matches with the channel measurements we made in different indoor environments. As the derivation of an analytical expression for the BER in a multipath channel and in the presence of multiuser interference is very complex, we used Monte-Carlo simulations to assess the performance of the different techniques in CM3 channels and validated our simulations by comparing them with the CF method which had been verified in [1] for the case of the AWGN channels.

This paper is organized as follows. Section II gives a brief description of the TH-PPM and TH-BPSK UWB system models and the decision statistics of the receiver under the AWGN and CM3 channels. The CF method applied to the TH-PPM and TH-BPSK in AWGN channel is introduced in section III. Then, section IV gives an overview of all parameters and assumptions used in our simulations. The results of the simulations and their analysis are then provided in section V. Finally, some conclusions are given in section VI.

II. System Model

In this section, we will describe the characteristics of the system. The TH-PPM transmitted by the kth user is represented as in [2], [3] by

$$S^{(k)}_{TH-PPM}(t) = \sqrt{E_g} \sum_{j=-\infty}^{+\infty} p(t - jT_f - c^{(k)}_j T_c - \delta d^{(k)}_{\lfloor j/N_s \rfloor}). \quad (1)$$

The TH-BPSK and BPSK-BPSK UWB signals can be written as

$$S^{(k)}_{TH-BPSK}(t) = \sqrt{E_g} \sum_{j=-\infty}^{+\infty} d^{(k)}_{\lfloor j/N_s \rfloor} p(t - jT_f - c^{(k)}_j T_c) \quad (2)$$

$$S^{(k)}_{BPSK-BPSK}(t) = \sqrt{E_g} \sum_{j=-\infty}^{+\infty} d^{(k)}_{\lfloor j/N_s \rfloor} b^{(k)}_j p(t - jT_f) \quad (3)$$

Where $S^{(k)}(t)$ is the random process modeling the transmitted signal by the kth user and $p(t)$ is the signal pulse with pulse duration tp. The parameters used in these UWB models are the following:

- E_g is the energy transmitted for each pulse.

- N_s is defined as the length of the repetition code [5]. It is the number of pulses required to transmit a single data bit. Hence, the bit energy is $E_b = N_s E_g$.
- T_f is the frame duration, therefore the bit duration is $T_b = N_s T f$.
- $c_j^{(k)}$ is the TH code for the kth user, which takes random integer values in the interval $0 \leq c_j^{(k)} < N_h$, where N_h is the time hopping code length.
- T_c is the time hopping chip duration.
- δ is the PPM shift used to distinguish between data bits 0 and 1.
- $d_{\lfloor j/N_s \rfloor}^{(k)}$ is the binary information stream transmitted by the kth user. $d_{\lfloor j/N_s \rfloor}^{(k)} \in \{0, 1\}$ in UWB systems that use PPM for data modulation. For BPSK data modulation $d_{\lfloor j/N_s \rfloor}^{(k)} \in \{-1, 1\}$.
- $b_j^{(k)}$ is the BPSK code. It produces a polarization of the pulse and can take the value -1 or 1.

Different pulse waveforms have been proposed for impulse-based UWB systems such as the Gaussian pulse, the Rayleigh monocycle [6], Scholtz monocycle [2], the Hermite polynomial monocycle [9] and the Prolate-Spheroidal wave function pulse [10]. In this paper, we adopt the Scholtz monocycle which is the second derivative of the Gaussian pulse. It can be represented as in [11] by

$$p(t) = \sqrt{\frac{4\zeta R\epsilon_b}{3t_n N_s}} \left(\frac{t^2}{t_n^2} - 1\right) \exp\left(-\frac{t^2}{2t_n^2}\right) \quad (4)$$

where $\zeta = 1/\sqrt{\pi}\,\mathrm{kgm}^2\mathrm{s}^{-2}$, t_n defines the pulse duration, R is the input impedance and ϵ_b/N_s is the pulse energy.

We assume that N_u users are transmitting data asynchronously on a channel. User 1 is the user of interest and the other N_u - 1 users are considered as interfering users. The received signal can thus be modeled as

$$r(t) = S^{(1)}(t - \tau_1) * h^{(1)}(t) + \sum_{k=2}^{N_u} S^{(k)}(t - \tau_k) * h^{(k)}(t) + n(t) \quad (5)$$

where $*$ denotes the convolution operator, $\{\tau_k, k = 1, 2, ..., N_u\}$ represents a time shift which accounts for user asynchronism, $\{h^{(k)}(t), k = 1, 2, ..., N_u\}$ represents the kth user channel impulse response and $n(t)$ is the additive noise with two-sided power spectral density $N_0/2$.

As explained in the introduction, we consider two different channel models, the AWGN channel and the IEEE 802.15.3a standard model [8]. For the AWGN channel the channel impulse response can be written as

$$h(t) = \delta(t) \quad (6)$$

The IEEE 802.15.3a standard model is based on a modification of the Saleh-Valenzuela [12]. This model takes into account the clustering phenomena observed in several UWB channel measurements. According to [8], the channel impulse response can be described mathematically as

$$h_i(t) = X_i \sum_{l=0}^{L} \sum_{k=0}^{K} \alpha_{k,l}^i \delta(t - T_l^i - \tau_{k,l}^i) \quad (7)$$

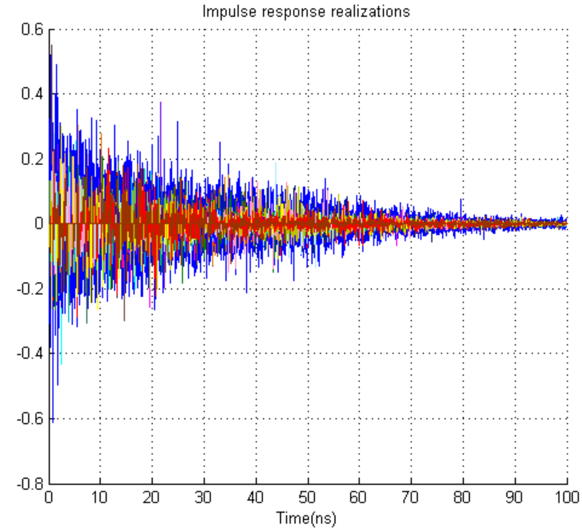

Fig. 1. 100 impulse responses based on CM3

where

- $\alpha_{k,l}^i$ are the multipath gain coefficients
- T_l^i is the delay of the l^{th} cluster
- $\tau_{k,l}^i$ is the delay of the k^{th} multipath component relative to the l^{th} cluster arrival time T_l^i
- X_i represents the log-normal shadowing, and i refers to the i^{th} realization

The distribution of cluster arrival time and the ray arrival time is exponential. The average power delay profile shows a double exponential decay and the fading statistics are log-normally distributed. Each multipath replica is either positive or negative, each with the same probability. In [8], four different measurement environments were defined, namely CM1, CM2, CM3 and CM4.

- CM1 describes a LOS (Line Of Sight) channel with TX-RX (Transmitter-Receiver) distance between 0 and 4 m.
- CM2 describes a NLOS (Non Line Of Sight) channel with TX-RX distance between 0 and 4 m.
- CM3 describes a NLOS channel with TX-RX distance between 4 and 10 m.
- CM4 describes an environment with strong delay dispersion, resulting in delay spread of 25 ns.

In our work, we have generated and saved 100 channels based on CM3 as it provided the best fit with our real indoor channel measurements. In the simulations, each user is assigned randomly one of these channels. The impulse response of these 100 channels is shown in Fig. 1. The receiver architecture used in this work is similar to the one used in [11] where a correlation receiver with a locally generated template is used. The receiver adopts $v(t) = p(t) - p(t - \delta)$ as a template when PPM is used for data modulation and it adopts $v(t) = p(t)$ as a template when BPSK is used instead. The pulses are shifted accordingly to the spreading sequence $\{c_j\}$ and coherently combined when TH is used for code modulation. When BPSK is used for code modulation the pulses are polarized according to the $\{b_j\}$ sequence and are coherently combined. In both cases the resulting signal $r(t)$ is correlated with the locally generated template.

III. Bit Error Probability Analysis

Different approaches were used in previous work to model the MAI (Multiple Access Interference). In [2], [3], [6] the MAI was modeled as Gaussian process for the random hopping characteristics of the TH-PPM UWB. In [5], they proposed a method to evaluate the BER performance of TH-PPM in the presence of MAI and AWGN channel, based on Gaussian Quadrature Rules (GQR). In [1], a characteristic function (CF) method was proposed for calculating the bit-error probability of TH UWB systems with MAI and in AWGN channel. In [1], [5], [7], the comparison between theoretical analysis and simulation shows the non validity of the Gaussian approximation. In our work, we will use the characteristic function method presented in [1] to validate our simulations in an AWGN channel.
The BER of TH-PPM UWB system is given in [1] by

$$P_{TH-PPM} = \frac{1}{2} - \frac{1}{\pi}\int_0^\infty \frac{\sin(A_1 N_s \tilde{R}(0) w)}{w}\phi_i(w) e^{-\sigma_n^2 w^2/2} dw \tag{8}$$

where

- A_1 represents the channel attenuation for the user of interest.
- $\tilde{R}(0)$ is the correlation of the template with a time-shifted pulse.
- $\phi_i(w)$ is the CF of the total interference in the TH-PPM system.
- $e^{-\sigma_n^2 w^2/2}$ is the CF of a Random Variable (RV) n with zero mean and variance $\sigma_n^2 = N_0 N_s^2 \tilde{R}(0)/E_b$.

On the other hand, for TH-BPSK UWB systems the BER is given in [1] by

$$P_{TH-BPSK} = \frac{1}{2} - \frac{1}{\pi}\int_0^\infty \frac{\sin(A_1 N_s w)}{w}\phi_i(w) e^{-\sigma_{n-BPSK}^2 w^2/2} dw \tag{9}$$

where

- A_1 represents the channel attenuation for the user of interest.
- $\phi_i(w)$ is the CF of the total interference in the TH-PPM system.
- $e^{-\sigma_{n-BPSK}^2 w^2/2}$ is the CF of a Random Variable (RV) n with zero mean and variance $\sigma_{n-BPSK}^2 = N_0 N_s^2 / 2E_b$.

IV. Simulation Assumptions and Parameters

All the simulations in this paper were conducted using the parameters listed in Table I.

As mentioned before, the simulations were conducted for both the AWGN and the CM3 channel. For the CM3 channel each user is assigned a random channel. We assume that all the users' powers are equal. The multiuser codes for time hopping are chosen randomly. Using Monte Carlo simulation, the simulations were performed until at least 200 bit errors had been detected or when 1,000,000 bits had been transmitted.

TABLE I
Parameters of TH-PPM and TH-BPSK systems

Parameter	Symbol	Value
Pulse duration	T_p	2 ns
PPM delay	δ	2 ns
Frame duration	T_f	100 ns
Chip duration	T_c	2 ns
Number of chips per frame	N_h	4,8
Number of users	N_u	10
Repetition code length	N_s	2, 4, 8, 16

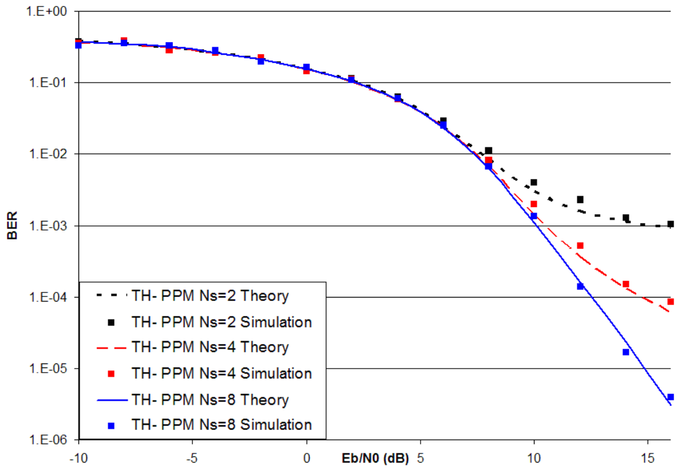

Fig. 2. BER in AWGN channel vs. E_b/N_0 of a TH-PPM UWB system with nine interfering users for $N_s = 2$, 4 and 8

V. Simulation Analysis

In this section the results obtained with the analytic expressions of the BER for TH-PPM and TH-BPSK in an AWGN channel are compared to the ones derived from the simulations. The simulation results of the system in multipath environment (CM3 channel) will be also presented.

In Fig. 2, the solid curves represent the average BER results of TH-PPM systems obtained by the CF method with a

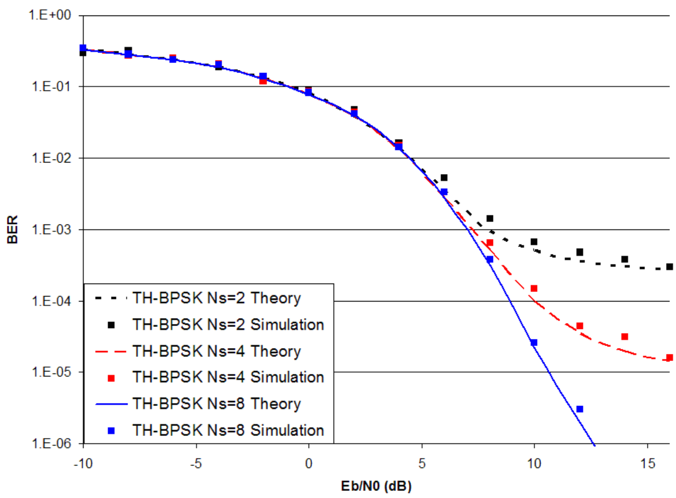

Fig. 3. BER in AWGN channel vs. E_b/N_0 of a TH-BPSK UWB system with nine interfering users for $N_s = 2$, 4 and 8

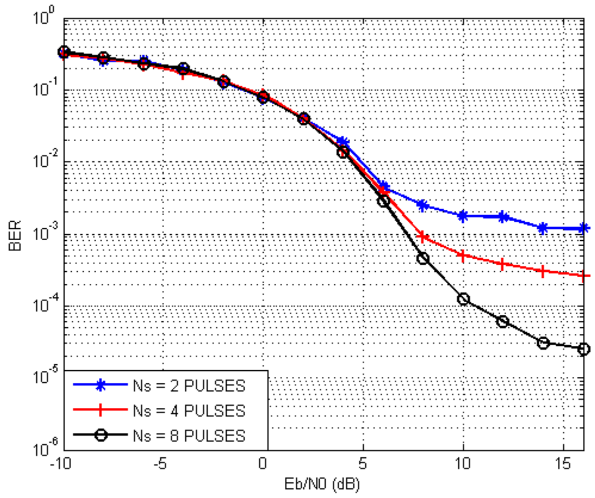

Fig. 4. BER in AWGN channel vs. E_b/N_0 of BPSK-BPSK UWB system with nine interfering users for $N_s = 2$, 4 and 8

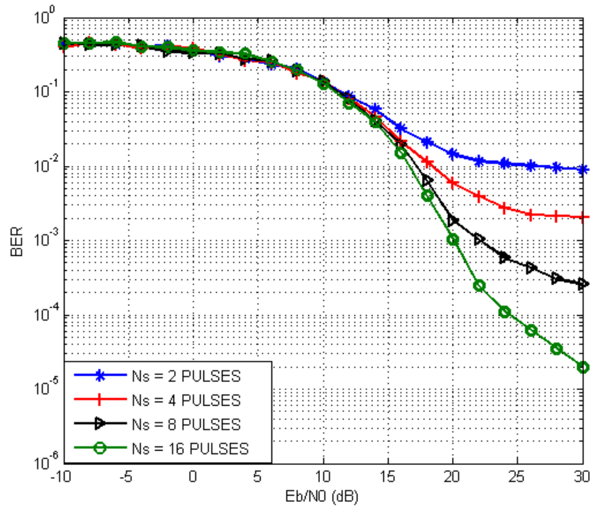

Fig. 5. BER in CM3 channel vs. E_b/N_0 of a TH-PPM UWB system with nine interfering users for $N_h = 4$, $N_s = 2$, 4, 8 and 16

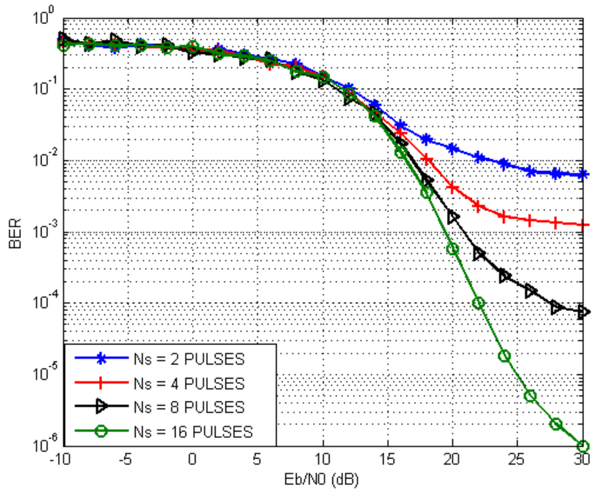

Fig. 6. BER in CM3 channel vs. E_b/N_0 of a TH-PPM UWB system with nine interfering users for $N_h = 8$, $N_s = 2$, 4, 8 and 16

repetition code of 2, 4 and 8 pulses and the squares represent the average BER obtained by Monte Carlo simulations. It is observed that the results achieved by the CF method are very close to the simulated ones. As expected, we can notice that the BER performance is improved when increasing the length of the repetition codes. Fig. 3 shows the BER results obtained by the CF method for the TH-BPSK system and the BER curves obtained by Monte Carlo simulations. As for TH-PPM systems, results achieved by the CF method and simulations are very close. In Fig. 4, the BER simulations for BPSK-BPSK are shown for different lengths of the repetition code, for $N_s = 2$, 4 and 8. As expected, the performance is improving with increasing the number of pulses per bit. In comparing Fig. 2, Fig. 3 and Fig. 4, it can be noticed that for the same length of repetition code TH-BPSK and BPSK-BPSK provide a better performance than TH-PPM. This can be explained by the fact that an antipodal modulation system has a 3 dB gain over the orthogonal modulation system in an AWGN channel [13].

Fig. 5 shows the average BER for TH-PPM UWB communication system in the presence of nine interfering users over multipath channels of type CM3 versus the signal to noise ratio for different lengths of repetition code N_s. Fig. 6 shows the same simulations when eight chips instead of four are used per frame for TH. Observing these figures it can be noticed that, as in the case of AWGN channel, increasing the number of pulses per bit, as well as using higher number of chips per frame for TH, results in better performance. Fig. 7 and Fig. 8 present simulations for the same conditions as Fig. 5 and Fig. 6, respectively, but in this case, for TH-BPSK UWB system. We note that the performance for TH-BPSK UWB systems can also be improved by increasing the length of the repetition code as well as increasing the number of chips per frame. In Fig. 9, the BER for BPSK-BPSK is shown for different lengths of the repetition code, $N_s = 2$, 4, 8, and 16. As expected, the performance is improving with increasing the number of pulses per bit. From Fig. 9 we note that BPSK-BPSK has better performance than TH-PPM, presented in Fig. 5 and Fig. 6. This is due to the fact that BPSK is a more efficient modulation scheme than PPM. Comparing Fig. 7 with Fig. 9, it can be noticed that for $N_s = 2$, 4 and 8 BPSK-BPSK has similar performance than TH-BPSK with $N_h = 4$. However for $N_s = 16$, BPSK-BPSK results in a better performance than TH-BPSK with $N_h = 4$. The comparison between Fig. 8 and Fig. 9 shows that for $N_s = 2$, 4 and 8 TH-BPSK with $N_h = 8$ has better performance than BPSK-BPSK and they have similar performance for $N_s = 16$. Different modulation schemes for $N_s = 16$ pulses are summarized in Fig. 10. The results confirm the previous observations showing that modulation schemes with BPSK for data modulation give better results than the ones using PPM. Furthermore, Fig. 10 shows that for $N_s = 16$, BPSK-BPSK is better than TH-BPSK when 4 chips per frame are used and gives similar performance

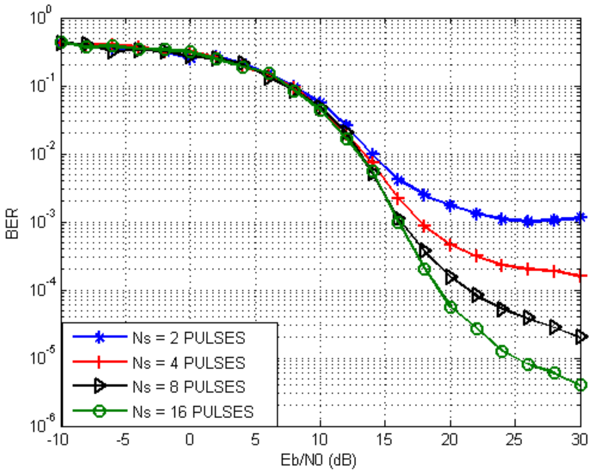

Fig. 7. BER in CM3 channel vs. E_b/N_0 of a TH-BPSK UWB system with nine interfering users for $N_h = 4$, $N_s = 2$, 4, 8 and 16

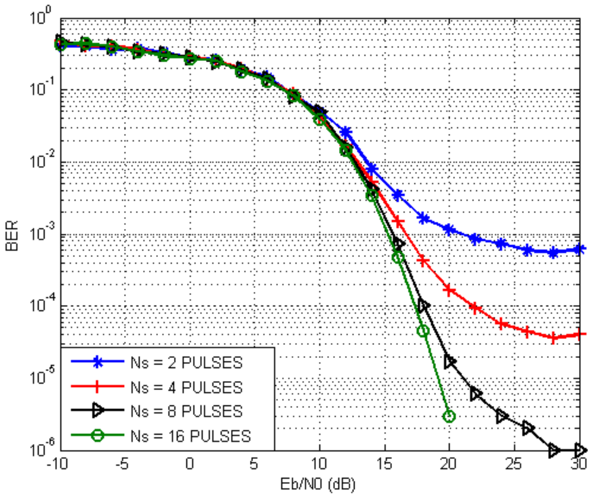

Fig. 8. BER in CM3 channel vs. E_b/N_0 of a TH-BPSK UWB system with nine interfering users for $N_h = 8$, $N_s = 2$, 4, 8 and 16

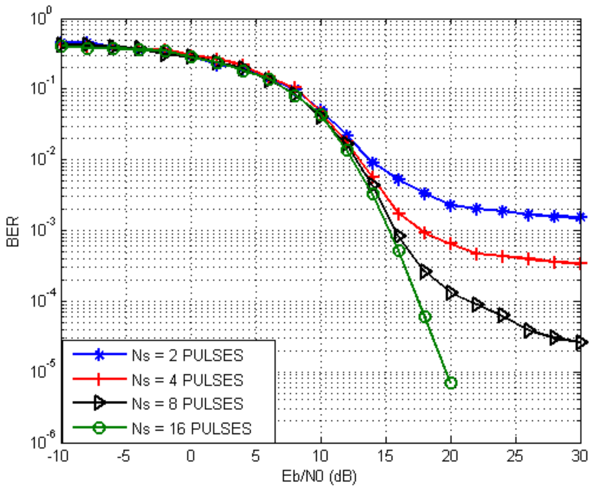

Fig. 9. BER in CM3 channel vs. E_b/N_0 of a BPSK-BPSK UWB system with nine interfering users for $N_s = 2$, 4, 8 and 16

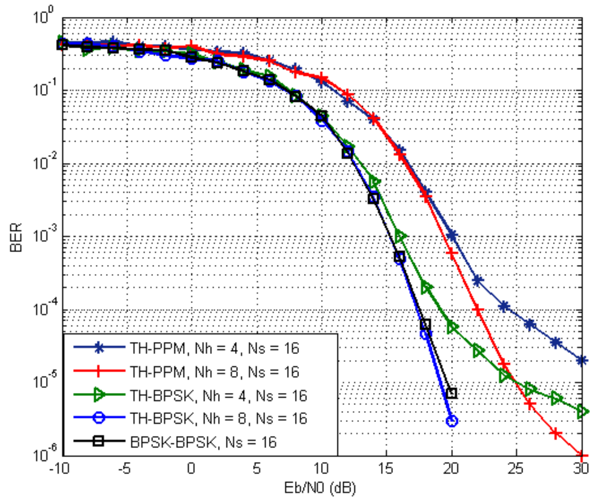

Fig. 10. BER in CM3 channel vs. E_b/N_0 for different modulation schemes in a UWB system with nine interfering users for $N_s = 16$

as TH-BPSK when 8 chips per frame are used. The plots of the simulation results in CM3 channel and in the presence of interfering users show similar behaviors as the ones obtained for the AWGN channel. We conclude that, for small values of E_b/N_0 (E_b/N_0 < 10 dB) the background noise is dominating the performance, while for medium values of E_b/N_0 (10 dB < E_b/N_0 < 20 dB) the modulation technique becomes more important and for large values of E_b/N_0 (E_b/N_0 > 20 dB) the interference is dominating and the curves are showing saturation in BER performance. Comparing the simulations in CM3 channel and the theoretical BER in an AWGN channel we notice that in a multipath environment and for medium values of E_b/N_0 (10 dB < E_b/N_0 < 20 dB), the performance is degraded by approximately 8 dB.

VI. Conclusion

In this work, the BER performance of different impulse-based multiple access and modulation techniques in AWGN and CM3 channels were investigated. Results of Monte Carlo simulations in AWGN channel were compared to the CF method and the simulation outcomes showed a good agreement with the theoretical results. Simulations under the same conditions were performed for the indoor multipath (CM3) channel. The performance of TH-BPSK, TH-PPM and BPSK-BPSK schemes in CM3 channels showed reduced performance but similar behavior as in AWGN channels, wherein with the increasing length of the repetition code, as well as the number of chips per frame, the BER performance is improving. It is also observed that BPSK-BPSK, which has a lower implementation complexity than TH-PPM and TH-BPSK, presents in a multipath CM3 channel similar performances as TH-BPSK and superior performance over TH-PPM.

Acknowledgment

The authors are grateful to the Swiss National Science Foundation (http://www.snsf.ch) who supports this work under grant 200020-113472.

REFERENCES

[1] B. Hu and N. C. Beaulieu, "Accurate evaluation of multiple-access performance in th-ppm and th-bpsk uwb systems," *IEEE Transactions on Communications*, vol. 52, no. 10, pp. 1758–1766, Sep. 2004.

[2] R. A. Scholtz, "Multiple access with time-hopping impulse modulation," in *Military Communications Conference*, vol. 2, Boston, MA, USA, Oct. 1993, pp. 447–450, invited Paper.

[3] M. Z. Win and R. A. Scholtz, "Ultra-wide bandwidth time-hopping spread-spectrum impulse radio for wireless multiple-access communications," *IEEE Transactions on Communications*, vol. 48, no. 4, pp. 679–691, Apr. 2000.

[4] M. L. Welborn, "System considerations for ultra-wideband wireless networks," in *IEEE Radio and Wireless Conference*, Boston, MA, USA, Aug. 2001, pp. 5–8.

[5] G. Durisi and S. Benedetto, "Performance evaluation of th-ppm uwb systems in the presence of multiuser interference," *IEEE Communications Letters*, vol. 7, no. 5, pp. 224–226, May 2003.

[6] L. Zhao and A. M. Haimovich, "Performance of ultra-wideband communications in the presence of interference," *IEEE Journal on Selected Areas in Communications*, vol. 20, no. 9, pp. 1684–1692, Dec. 2002.

[7] G. Durisi and G. Romano, "On the validity of gaussian approximation to characterize the multiuser capacity of uwb th ppm," in *IEEE Conference on Ultra Wideband Systems and Technologies*, Baltimore, MD, USA, May 2002, pp. 157–161.

[8] J. R. Foerster, M. Pendergrass, and A. F. Molisch, "A channel model for ultrawideband indoor communication," *IEEE Transactions on Wireless Communications*, vol. 10, no. 6, pp. 14–21, Dec. 2003.

[9] M. Ghavami, L. B. Michael, S. Haruyama, and R. Kohno, "A novel uwb pulse shape modulation system," *Wireless Personal Communications, Kluwer Academic Publishers*, vol. 23, no. 1, pp. 105–120, Oct. 2002.

[10] B. Parr, B. Cho, K. Wallace, and Z. Ding, "A novel ultra-wideband pulse design algorithm," *IEEE Communications Letters*, vol. 7, no. 5, pp. 219–221, May 2003.

[11] R. Merz, C. Botteron, and P.-A. Farine, "Performance of an impulse radio communication system in the presence of gaussian jitter," in *IEEE International Conference on Ultra-Wideband*, Singapore, Sep. 2007.

[12] A. A. Saleh and R. A. Valenzuela, "A statistical model for inddor multipath propagation," vol. SAC-5, no. 2, pp. 128–137, Feb. 1987.

[13] S. Haykin, *Digital Communications*. John Wiley & Sons, 1988.